Time reversed elastic nonlinearity diagnostic applied to mock osseointegration monitoring applying two experimental models

Jacques Rivière,[a] Sylvain Haupert, and Pascal Laugier
Université Pierre et Marie Curie, Université Paris 06, CNRS Unité Mixte de Recherche 7623, Laboratoire d'Imagerie Paramétrique, F-75006, Paris, France

T. J. Ulrich, Pierre-Yves Le Bas, and Paul A. Johnson
EES-17, Los Alamos National Laboratory, Los Alamos, New Mexico 87545

(Received 12 April 2011; revised 7 December 2011; accepted 17 January 2012)

This study broadens vibration-like techniques developed for osseointegration monitoring to the nonlinear field. The time reversed elastic nonlinearity diagnostic is applied to two mock models. The first one consists of tightening a dental implant at different torques in a mock cortical bone; the second one allows one to follow glue curing at the interface between a dental implant and a mock jaw. Energy is focused near the implant interface using the time reversal technique. Two nonlinear procedures termed pulse inversion and the scaling subtraction method, already used successfully in other fields such as contrast agents and material characterization, are employed. These two procedures are compared for both models. The results suggest that nonlinear elasticity can provide new information regarding the interface, complementary to the linear wave velocity and attenuation. The curing experiment exhibits an overall low nonlinear level due to the fact that the glue significantly damps elastic nonlinearity at the interface. In contrast, the torque experiment shows strong nonlinearities at the focus time. Consequently, a parallel analysis of these models, both only partially reflecting a real case, enables one to envisage future *in vivo* experiments. [DOI: 10.1121/1.3683251]

PACS number(s): 43.25.Dc [ROC] Pages: 1922–1927

I. INTRODUCTION

Monitoring of osseointegration after total hip/knee replacement or dental implant sealing remains a challenge. X-ray based techniques, which are broadly applied along with clinical examinations, suffer from low resolution.[1] In addition, x-ray methods are less certain in light of the high reflection of metal prostheses.[2,3] This has lead to much research aimed at developing new techniques to reduce x-ray dose[4] and to minimize scattering.

In the 1990s, vibration analysis based techniques began to be developed.[5–9] These noninvasive and non-damaging techniques, which do not involve ionizing radiation, consist of monitoring the resonance frequency and/or damping, respectively, related to macroscopic stiffness and attenuation at the interface. Numerous *in vitro* and *in vivo* studies followed, showing mixed correlations with parameters such as insertion torque,[10,11] the bone implant contact (BIC, obtained from histomorphometry[12] or micro-computed tomography,[10,11] and the peri-implant bone elastic modulus (obtained from nano-indentation measurements).[13] Thus these tools still remain generally unproven for *in vivo* loose prostheses.[14–16]

Measurement of nonlinear elasticity has been widely developed over the last two decades for non-destructive evaluation of industrial materials and solid Earth materials.[17] Such nonlinearity likely comes from frictional effects and/or clapping sources at an interface, such as micro-cracks or disbonds typically, providing information on the contact integrity and complementing linear elasticity measurements.[18,19] To our knowledge, three groups have attempted measurement of nonlinear parameters at an interface bone/hip prosthesis (bone mock model,[20] *in vitro*[21] or *in vivo*).[9,22] In these studies, the system is driven at a single frequency f and harmonics are detected at $2f$ and $3f$ if the prosthesis is loose. In particular, the *in vivo* study conducted by Georgiou *et al.*,[22] which compares x-ray radiographs with linear and nonlinear elastic measurements, presents promising results. However, enhancement of signal to noise ratio in the measurement could improve the method sensitivity. Furthermore, most of these studies are only conducted for extreme cases of stability. Information over the entire osseointegration process, from the very loose to the well-secured case, would therefore be useful to complete our knowledge on the subject.

In the study reported here, we employ two signal processing approaches to extract the nonlinear behavior, termed pulse inversion (PI) and the scaling subtraction method (SSM), respectively. These were first developed to study the highly nonlinear behavior of bubbles (notably for contrast agent studies.[23] The PI procedure is performed by successively sending two pulses the polarity of which is inverted. The sum of the two responses, which is equal to zero in a linear system, adds even harmonics and suppresses the odd harmonics (fundamental component included) in the presence of weak acoustic/elastic nonlinearity.[24] On the other hand, the SSM procedure consists of successively sending two pulses the amplitude of which is different (one low amplitude, assumed linear, one larger amplitude assumed nonlinear). By rescaling

[a]Author to whom correspondence should be addressed. Electronic mail: riviere_jacques@yahoo.fr

both responses and computing the difference, the full nonlinearity is extracted.[25] These methods (and combination of both) are widely used in medical ultrasonic imaging using contrast agents and make the extraction of the nonlinear component easier compared to the traditional harmonic extraction.[24,26,27] Further, the PI procedure allows one to use a wide frequency band, where the fundamental and second harmonic components can overlap.[23] We apply the preceding signal processing approaches in combination with time reversal[28] (TR), an approach termed time reversed elastic nonlinearity diagnostic (TREND), part of the tool box known as time reversal nonlinear elastic wave spectroscopy and developed over the last decade as a new approach to detect defects in industrial materials,[29,30] landmine location,[27] rock characterization,[31] and more recently for tooth imaging.[32] Time reversal provides the means to focus energy at a desired location with large amplitudes, allowing very localized detection of nonlinear properties. Moreover, as high strain amplitude is only located at the focal point, weaker excitation at the source transducers is required to obtain an equivalent strain amplitude compared to unfocused methods; this reduces unwanted nonlinearities coming from the source or from associated source electronics.[27] Finally, TR allows one to focus energy with a random location, i.e., chosen convenient, of ultrasonic sources compared to traditional focusing methods (e.g. high-intensity focused ultrasound).

In the following, we report the first application of TREND using PI and SSM to osseointegration monitoring with the goal of ultimately applying similar methods *in vivo*.

II. EXPERIMENT

A dental implant/mock bone interface is investigated employing two different ways of mimicking osseointegration. The first experiment consists in tightening a dental implant [4.8 mm diameter, SwissPlus tapered from Zimmer (Carlsbad, CA, USA)] at different torques into a sample of mock cortical bone [short fiber filled epoxy sheet (76 mm × 18 mm × 2 mm) from Sawbones (Malmö, Sweden)] (Fig. 1). The mock cortical bone has elastic, dissipative, and density properties close to cortical bone (anisotropy included). However, no information regarding the nonlinear elastic properties is given by the manufacturer. In the second approach, glue curing is monitored at the interface between a mock jaw and the same implant. Wood glue (Elmer's, Columbus, USA) is selected to obtain a slow progressive curing with no change in temperature. The mock jaw was previously made by bonding a mock cortical bone (92 mm × 26 mm × 2 mm) to a mock trabecular bone (Cellular rigid polyurethane foam, diameter = 30 mm, h = 20 mm, from Sawbones) applying epoxy. Like mock cortical bone, the mock trabecular bone has a density as well as macroscopic linear elastic and dissipative properties close to that of human trabecular bone. Also, sheet-like samples are chosen for experimental ease: We would expect similar results with cylindrical samples for example, closer in geometry to *in vivo* conditions.

The experimental setup shown in Fig. 1(b) is composed of a bench vice, with eight piezoceramics bonded using epoxy. The mock cortical bone or the mock jaw is clamped in the vice for "torque" or "glue" experiments, respectively. A laser Doppler vibrometer (Polytec OFV-303 with OFV-3001 controller and VD-02 velocity decoder) is used to measure axial out-of-plane velocity on the implant ring. The vice acts as a highly scattering medium to maximize the focus.[33] It also provides the means to bond a large number of transducers to succeed in an efficient focus without affecting the sample.

The experimental protocol is described as follows [Fig. 1(a)]. Impulse responses (over a limited frequency band) are collected for each of the eight source-receiver paths, i.e., between each piezoceramic and the rim of the implant where the laser is pointed. The impulse responses are obtained in the following manner. A swept-sine source $e(t)$ (75–125 kHz) is used for excitation of each piezoceramic consecutively. Each recorded signal $s_n(t)$ obtained with the laser (with n, the transducer index ranging from 1 to 8) is cross-correlated with the input signal,

$$r_n(t) = s_n(t) * e(-t) \tag{1}$$

where $r_n(t)$ is proportional to the system impulse responses $h_n(t)$,[17] and the * symbol is the convolution operator. The frequency band is selected to maximize the signal to noise ratio of the laser vibrometer. At the same time, the frequency

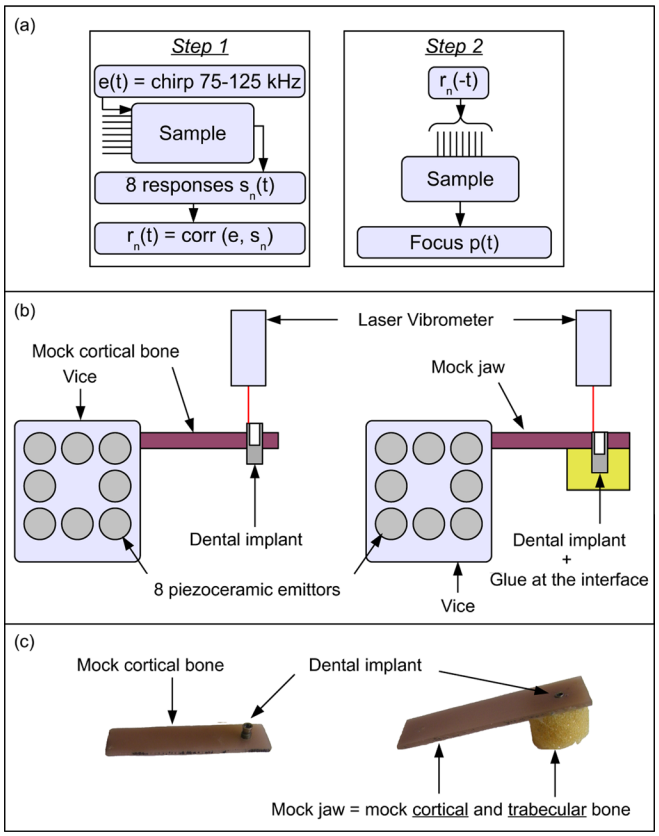

FIG. 1. (Color online) (a) Time reversal protocol. Step 1 is the "learning" step where the 8 impulse responses between each piezoceramic and the ring of the implant are obtained (the laser points to the ring). Step 2 is the time reverse and focus step. (b) Schematic representation of the experimental device. On the left, setup associated with the "torque" experiment. On the right, setup associated with the glue curing. (c) Photos of the two mock samples.

band is chosen to be narrow enough to avoid the overlapping of the fundamental component with second harmonic. The second step is composed of focusing the energy onto the implant employing the virtual source method of time reversal ("reciprocal TR"). In this manner, the eight $r_n(t)$ are time-reversed and emitted simultaneously from the piezoceramics. Typical foci are displayed in Fig. 2. To apply both PI and SSM procedures, step 2 is repeated four times, sending successively $r_n(-t)$, $-r_n(-t)$, $r_n(-t)/4$ and $-r_n(-t)/4$, giving, respectively, $p_1(t)$ to $p_4(t)$ foci.

The nonlinear components for PI and SSM are, respectively, obtained in the following way (Fig. 2):

$$\kappa^{pi}(t) = p_1(t) + p_2(t), \tag{2}$$

$$\kappa^{ssm}(t) = p_2(t) - 4p_4(t). \tag{3}$$

The combination $\kappa^{pi}_{lowamp}(t) = p_3(t) + p_4(t)$ gives the PI component at a low amplitude excitation [Fig. 2(b)]. The combination $p_1(t) - 4p_3(t)$, which could also be used for the SSM component, gives very similar results to the one obtained with equation 3 (data not shown).

III. RESULTS

We observe in Fig. 3 the creation of higher harmonics when the strain amplitude reaches a maximum at the focus time. The focus obtained for the component $\kappa^{pi}_{lowamp}(t)$ is very weak in amplitude, confirming the hypothesis of a linear regime for the weakest amplitude excitation [Fig. 3(b)].

A. Normalization

The focusing energy changes during torque and curing experiments [Figs. 4(a) and 5(a)], leading as expected, to higher nonlinear components κ^i (with $i = pi$ or ssm) with larger focusing energy. Therefore these two nonlinear components, composed of different harmonics, are normalized to take into account changes in the focusing energy. This normalization is dependent on the nonlinearity type.[34] A purely

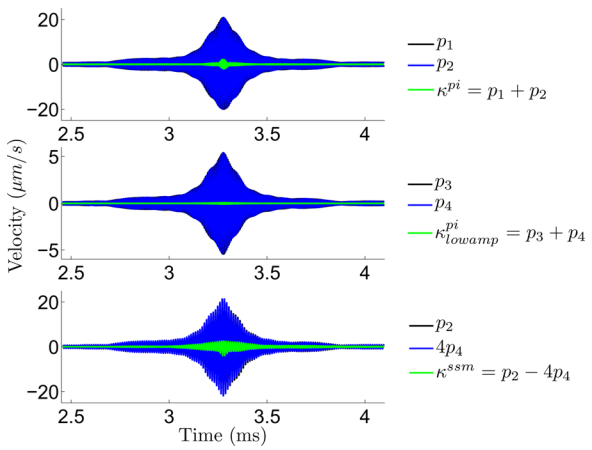

FIG. 2. (Color online) Time foci measured at 10N · cm and nonlinear components extracted from these foci vs time. (a) Recorded signals p_1 and p_2, as well as the nonlinear component κ^{pi}. (b) Recorded signals p_3 and p_4, as well as the nonlinear component κ^{pi}_{lowamp}. (c) Recorded signals p_2 and p_4, the latter being rescaled by a factor 4, and the nonlinear component κ^{ssm}.

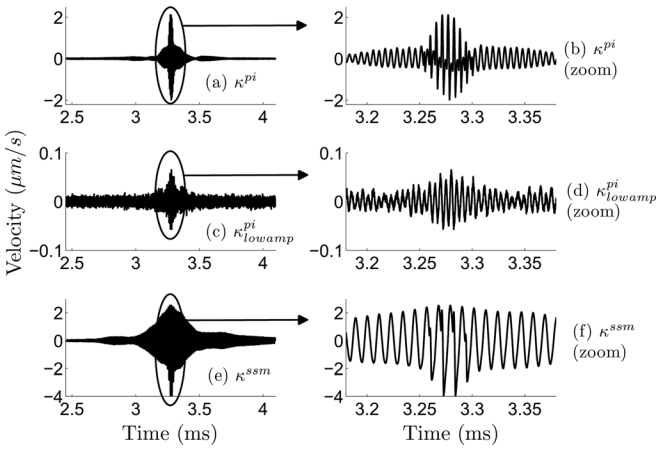

FIG. 3. Extracted nonlinear components at 10 N · cm vs time and respective zooms around the focal time. (a) Nonlinear component κ^{pi} calculated from the Eq. (2). (b) Nonlinear component κ^{pi}, zoom around the focal time. Note the strong distortion at the focal time. (c) Nonlinear component κ^{pi}_{lowamp}. Note the weak amplitude at the focal time, revealing a residual nonlinearity. (d) Nonlinear component κ^{pi}_{lowamp}, zoom around the focal time. (e) Nonlinear component κ^{ssm} calculated from the Eq. (3). (f) Nonlinear component κ^{ssm}, zoom around the focal time. Note the strong distortion at the focal time.

hysteretic nonlinearity leads to no even harmonics and a square power dependence for all odd harmonics. A classical nonlinearity, i.e., following Landau theory,[35] leads to both even and odd harmonics, each mth harmonic having a m-power dependence. In this study, due to the presence of both even and odd harmonics in the responses with no predominance of odd harmonics (Fig. 6), we assume the system to be primarily described by a classical nonlinearity. Thus the normalized nonlinear parameter ν^i_m (with the integer $m \geq 2$) is calculated as follows:

$$\nu^i_m = max\left(\kappa^i_{mf}\right)/max\left(p^m_{1,f}\right) \tag{4}$$

where κ^i_{mf} is the filtered part of κ^i around the mth harmonic and $p^m_{1,f}$ is the filtered part of p_1 around the fundamental frequency, to the mth power.

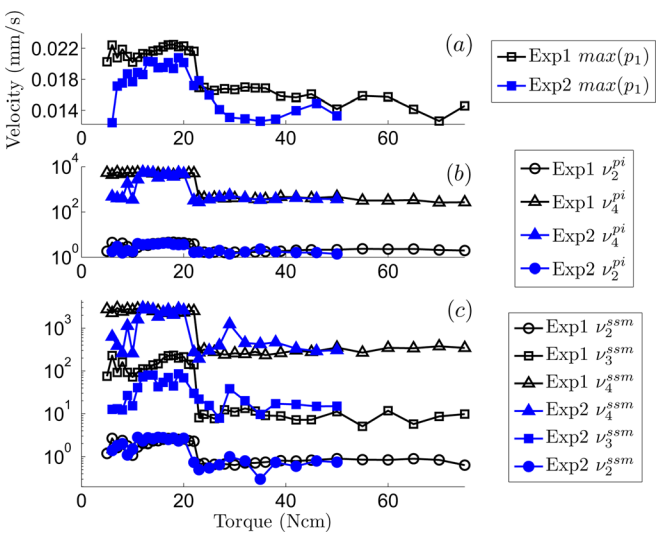

FIG. 4. (Color online) Evolution of foci's maxima and associated nonlinear parameters vs torque, expressed in N · cm, for two experiments. (a) Maximum of the focus p_1. (b) Evolution of nonlinear parameters ν^{pi}_2 and ν^{pi}_4. (c) Evolution of nonlinear parameters ν^{ssm}_2 to ν^{ssm}_4.

B. Evolution with torque and glue curing

The maximum of focusing signal p_1, as well as the evolution of nonlinear parameters ν_m^i, are presented in Figs. 4 and 5 for the torque and the glue experiment, respectively. Moreover, in Fig. 4, two distinct experiments of torque change are presented. The behavior is similar for both experiments, revealing a quite good consistency. However, the maximum tightening reached for both experiments is different (50 and 75 N · cm). Indeed with the implant's tightening being destructive for the mock cortical bone, the experiment is terminated when the ultimate stress is reached, and a new mock cortical bone is used for the next experiment. This different ultimate stress could be explained by a slightly different perforation diameter in the mock cortical bone during the preparative process. Indeed a few tenths of a millimeter could probably be enough to observe this difference. A second explanation is linked to the tightening velocity, proportional to the strain rate, which is not accurately controlled in the experiment. A rapid tightening velocity could actually be the reason for an early rupture.

Comparing Figs. 4(a) and 5(a), we see that the focal maximum decreases by few percent in the case of the torque experiment while it increases by a factor more than 2 in the curing experiment. This point will be interpreted in the discussion.

Nonlinear parameters ν_m^{pi} and ν_m^{ssm} are displayed, respectively, in Figs. 4(b) and 4(c) for the torque experiment. Five harmonics are observed in the signals (only three are displayed for figure clarity) and as expected, only even harmonics can be extracted from the PI procedure. A sudden decrease of the nonlinear components occurs around 20-23 N · cm. Further, this trend is approximately the same as the one observed for the focus maximum [Fig. 4(a)].

For the curing experiment, only ν_2^{pi} is shown, as higher harmonics do not emerge from the noise level. For SSM, even the second harmonic does not emerge (not plotted). In Fig. 5(b), the nonlinear component ν_2^{pi} increases during the three first hours of curing, attaining a maximum around the 15th hour, and then decreasing. A plateau is reached after roughly the 25th hour.

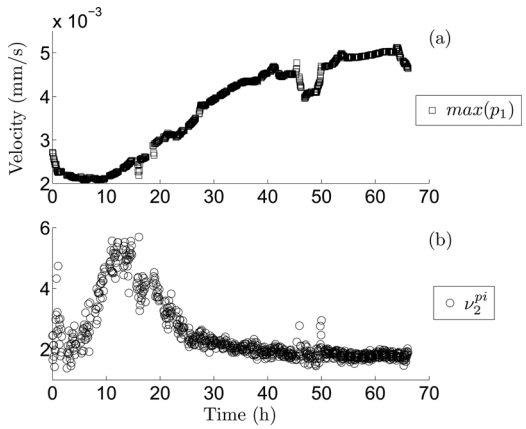

FIG. 5. (a) Evolution of the focus maximum p_1 vs curing time. (b) Evolution of the nonlinear parameter ν_2^{pi} vs curing time.

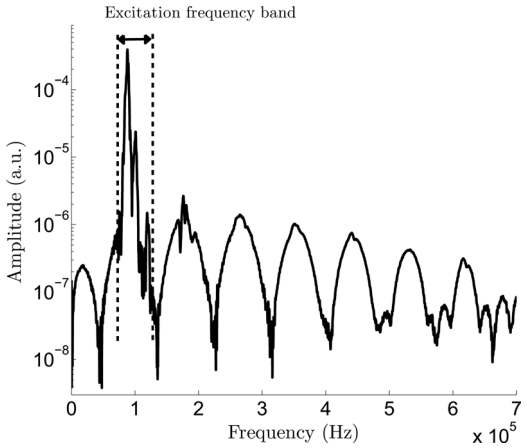

FIG. 6. Spectrum of the focus signal p_1 for a 10 N · cm-torque. We observe the presence of both odd and even harmonics without predominance of odd harmonics. This observation supports primarily a nonlinear "classical" regime that is taken into account for the normalization of κ parameters.

IV. DISCUSSION

A. Nonlinear evolution

Two separate experiments have been performed to mimic the osseointegration process. In the curing experiment (Fig. 5), we believe that the overall low nonlinear level is due to the fact that the glue significantly damps nonlinearity at the interface. We infer this because four harmonics are present in the torque experiment (Fig. 4), whereas only one is measurable during the curing. The nonlinear "sources" coming essentially from friction and stick/slip behaviors at the interface, the presence of the glue inhibits or at least attenuates these phenomena. In the same manner, characteristic clapping-type behaviors, which may also contribute to the observation of nonlinearity, are reduced by the glue.

At the onset of curing (Fig. 5), the primary contact is a viscous-like state, giving modest nonlinearity. As the glue cures, the nonlinearity increases, reaching a maximum around the 15th hour of curing. The nonlinearity then decreases smoothly until the curing is complete and the contact perfect. The curing time given by the manufacturer (24 h) coincides well with the beginning of the low stable nonlinear level. Thus we assume that a competition occurs between viscosity and nonlinear effects at the beginning of the curing, leading to modest nonlinearity when viscosity is high. This has to be confirmed by future experiments.

During the torque experiment, no implant motion was detectable by hand or visually during tightening except at very low torques (5–10 N · cm) and when the drop in response occurs around 20–23 N · cm, affecting both total [Fig. 4(a)] and nonlinear [Figs. 4(b) and 4(c)] components. Consequently, we presume the tightening from 22 to 23 or 20 to 21 N · cm suddenly leads to a more intimate contact.

B. Linear evolution

In both experiments, we would expect an increase of focused energy as the contact improves and wave energy traverses the contact more easily [Figs. 4(a) and 5(a)]. For the glue experiment [Fig. 5(a)], we effectively observe an

increase of the energy, the focused amplitude being multiplied by more than 2 during the curing. However, for torque experiment in Fig. 4(a), the focused amplitude decreases by few percentages. We believe that this amplitude drop is the result of the concurrent evolution of two different parameters during the torque increase. We assume that the expected increase in focused amplitude in response to the static stress increase at the interface is partly weakened by a change in the relative position of both objects (implant and plate), the implant being seated more deeply in the plate when the torque increases. We think that this change damps the energy of the eigenmodal frequencies of the implant which are contained in the usable frequency bandwidth. We checked this hypothesis by using a traditional screw instead of the dental implant (i.e., with different geometry), leading to much less energy in the frequency band. The main contribution in the frequency band is hence due to implant's modes. Thus we think that the relative vertical change between the plate and the implant during tightening reduces the energy of several eigenmodes of the implant, leading to a slight decrease of focused amplitude.

C. Comparison of both models

In the torque experiment, the actual interface (mock bone/metal implant) is studied but the tightening results in a progressively deeper implant, a phenomenon not present in the actual osseointegration process. This last feature is not present in the curing experiment, but a third component has to be present at the interface (the glue), highly reducing the nonlinear response. Finally, we may expect some intermediate conditions *in vivo* between some completely dry conditions (torque experiment) and highly viscous conditions (glue curing).

The ratio of elastic moduli is about 7 between both materials: Young's moduli are 110 and 16 GPa for titanium and cortical bone, respectively.[36,37] Thus for the torque experiment, tightening the metallic implant into a much less stiff material results in a plastic deformation, tapping the mock bone. This phenomenon may explain the abrupt transition observed around 20–23 N · cm. In a previous study,[19] a metal screw was tightened in an aluminum tapped plate (205 and 75 GPa for Young's moduli of steel and aluminium, respectively,[36] giving a 2.7 ratio), and extracted elastic parameters showed only smooth transition over a large torque range. No plastic deformation between these two similar materials was induced in this case. This aspect remains a limitation of the torque experiment used here to mimic the actual progressive osseointegration. Finally, both models show different limitations and only a comparative study allows to envisage what could be obtained *in vivo*.

D. Comparison of both methods

The PI method leads only to even harmonic amplitudes but has the advantage of completely eliminating the fundamental part of signal (κ^{pi} has no component at the fundamental frequency). This fact provides the means to use a larger frequency band with overlap of fundamental with second harmonic (not applied here to compare PI with SSM). On the other hand, the SSM allows one to obtain the entire nonlinear response as described by Bruno *et al.*[25] As this method allows to obtain the nonlinearity of all harmonics and at the fundamental frequency, it requires a narrower frequency band excitation to avoid that fundamental component and second harmonic overlap. Finally, we note that in the curing experiment, where nonlinearity is weak, we were unable to obtain a clear second harmonic for the SSM experiment. The reason why we could not extract any second harmonic remains unclear. One reason may be due to the fact that the same acquisition card's vertical range was kept for both high ($p_{1,2}$) or low ($p_{3,4}$) focusing, leading to lower signal to noise ratio. Beyond these observations, one has to keep in mind that other combinations could be carried out in future experiments to increase the signal to noise ratio. In particular, methods already used for medical ultrasonic imaging and combining PI and SSM procedures through two or more signals could lead in a more efficient extraction.[38]

E. Study limitations and perspectives

One limitation of the study is the fact that we hypothesize one nonlinearity type from the spectral content to extract normalized nonlinear parameters. The solution to overcome this limitation would be to perform the experiment at multiple amplitudes of excitation and to extract the true amplitude dependence. Indeed the true dependence may deviate from the classical nonlinearity without being detectable from the respective amplitudes of odd and even harmonics. Nevertheless, performing the experiment at multiple amplitudes of excitation and for multiple "osseointegration stages" remains highly time-consuming, and we chose to excite only at two amplitudes for that reason. The second limitation is the limited dataset presented in our study. It does not allow us to check the robustness of the technique or to provide a comprehensive uncertainty analysis of the evolution obtained all along the torque increasing and glue curing. The torque experiment could be performed twice, and results showed a similar trend for both experiments. However, the glue curing experiment has been performed only once: The result must then be taken with caution. Further experiments are needed to confirm the robustness of the techniques. Future experiments will also include some changes to avoid drawbacks observed with both experimental models (Sec. IV C). Finally, some more complex combinations will be used to increase the effectiveness of nonlinearity extraction (Sec. IV D).

V. CONCLUSION

In conclusion, this experiment expands vibration-like techniques developed for osseointegration monitoring to the nonlinear field. We present the nonlinearity evolution obtained through two experiments mimicking osseointegration, from the loose to the well-secured case. The time reversal technique allows one to focus energy at a desired location to extract local nonlinear elastic properties. Thus providing new information on the interface, we expect these methods could increase efficiency of future devices and ultimately enhance the decision support for clinicians. This

study will be carried on in the future by both *in vitro* and *in vivo* measurements.

ACKNOWLEDGMENTS

Authors would like to thank R. Guyer, J. TenCate, and E. Daub (Los Alamos National Laboratory) for fruitful discussions and comments. P.A.J. was supported by Institutional Support (LDRD) at the Los Alamos National Laboratory, and funds from CNRS France.

[1]T. Albrektsson, G. Zarb, P. Worthington, and A. R. Eriksson, "The long-term efficacy of currently used dental implants: a review and proposed criteria of success," Int. J. Oral Maxillofac. Implants **1**, 11–25 (1986).
[2]R. Bernhardt, D. Scharnweber, B. Muller, F. Beckmann, P. Thurner, H. Schliephake, P. Wyss, F. Beckmann, J. Goebbels, and H. Worch, "Comparison of microfocus-and synchrotron x-ray tomography for the analysis of osteointgration around Ti6Al4V implants," Eur. Cells Mater. **7**, 42–51 (2004).
[3]M. Sabo, S. Pollmann, K. Gurr, C. Bailey, and D. Holdsworth, "Use of co-registered high-resolutionand after screw insertion as a novel technique for bone mineral density determination along screw trajectory," Bone **44**, 1163–1168 (2009).
[4]J. Hainfeld, D. Slatkin, T. Focella, and H. Smilowitz, "Gold nanoparticles: a new X-ray contrast agent," Br. J. Radiol. **79**, 248–253 (2006).
[5]B. Dhoedt, D. Lukas, L. Muhlbradt, F. Scholz, W. Schulte, F. Quante, and A. Topkaya, "Periotest procedure—development and clinical-testing," Dtsch. Zahnaerztl. Z. **40**, 113–125 (1985).
[6]A. Rosenstein, C. Bulstrode, P. Smith, J. Cunningham, and A. Turner-Smith, "The differentiation of loose and secure femoral implants in total hip replacement using a vibrational technique:and pilot clinical study," Proc. Inst. Mech. Eng. **203**, 77–81 (1989).
[7]I. Denayer and G. Van der Perre, "Detection of hip stem loosening using vibration analysis," J. Biomech. **31**, 165–165 (1998).
[8]N. Meredith, D. Alleyne, and P. Cawley, "Quantitative determination of the stability of the implant-tissue interface using resonance frequency analysis," Clin. Oral Impl. Res. **7**, 261–267 (1996).
[9]R. Puers, M. Catrysse, G. Vandevoorde, R. Collier, E. Louridas, F. Burny, M. Donkerwolcke, and F. Moulart, "A telemetry system for the detection of hip prosthesis loosening by vibration analysis," Sens. Actuators, A **85**, 42–47 (2000).
[10]K. Akca, T. Chang, I. Tekdemir, and M. Fanuscu, "Biomechanical aspects of initial intraosseous stability and implant design: a quantitative micromorphometric analysis," Clin. Oral Implants Res. **17**, 465–472 (2006).
[11]I. Turkyilmaz, T. F. Tozum, C. Tumer, and E. N. Ozbek, "Assessment of correlation between computerized tomography values of the bone, and maximum torque," J. Oral Rehabil. **33**, 881–888 (2006).
[12]H. Schliephake, A. Sewing, and A. Aref, "Resonance frequency measurements of implant stability in the dog mandible: experimental comparison with histomorphometric data," Int. J. Oral Maxillofac. Surg. **35**, 941–946 (2006).
[13]W. Seong, J. Holte, J. Holtan, P. Olin, J. Hodges, and C. Ko, "Initial stability measurement of dental implants placed in different anatomical regions of fresh human cadaver jawbone," J. Prosthet. Dent. **99**, 425–434 (2008).
[14]C. Aparicio, N. R. Lang, and B. Rangert, "Validity and clinical significance of biomechanical testing of implant/bone interface," Clin. Oral Implants Res. **17**, 2–7 (2006).
[15]M. Atsumi, S. Park, and H. Wang, "Methods used to assess implant stability: Current status," Int. J. Oral Maxillofac. Implants **22**, 743–754 (2007).
[16]F. Javed and G. Romanos, "The role of primary stability for successful immediate loading of dental implants. A literature review," J. Dent. **38**, 612–620 (2010).
[17]R. Guyer and P. Johnson, *Nonlinear Mesoscopic Elasticity: The Complex Behaviour of Rocks, Soil, Concrete* (Wiley Vch Pub, Weinheim, 2009).
[18]W. Morris, O. Buck, and R. Inman, "Acoustic harmonic-generation due to fatigue damage in high-strength aluminum," J. Appl. Phys. **50**, 6737–6741 (1979).
[19]J. Riviere, G. Renaud, S. Haupert, M. Talmant, P. Laugier, and P. Johnson, "Nonlinear acoustic resonances to probe a threaded interface," J. Appl. Phys. **107**, 124901 (2010).
[20]A. Rowlands, F. Duck, and J. Cunningham, "Bone vibration measurement using ultrasound: Application to detection of hip prosthesis loosening," Med. Eng. Phys. **30**, 278–284 (2008).
[21]P. L. S. Li, N. B. Jones, and P. J. Gregg, "Vibration analysis in the detection of total hip prosthetic loosening," Med. Eng. Phys. **18**, 596–600 (1996).
[22]A. Georgiou and J. Cunningham, "Accurate diagnosis of hip prosthesis loosening using a vibrational technique," Clin. Biomech. **16**, 315–323 (2001).
[23]M. Averkiou, "Tissue harmonic imaging," Proc. IEEE Ultrason. Symp. **2**, 1563–1572 (2000).
[24]D. Simpson, C. Chin, and P. Burns, "Pulse inversion Doppler: A new method for detecting nonlinear echoes from microbubble contrast agents," UFFC IEEE **46**, 372–382 (2002).
[25]C. Bruno, A. Gliozzi, M. Scalerandi, and P. Antonaci, "Analysis of elastic nonlinearity using the scaling subtraction method," Phys. Rev. B **79**, 064108 (2009).
[26]P. Frinking, A. Bouakaz, J. Kirkhorn, F. T. Cate, and N. de Jong, "Ultrasound contrast imaging: current and new potential methods," Ultrasound Med. Biol. **26**, 965–975 (2000).
[27]A. Sutin, B. Libbey, L. Fillinger, and A. Sarvazyan, "Wideband nonlinear time reversal seismo-acoustic method for landmine detection," J. Acoust. Soc. Am. **125**, 1906–1910 (2009).
[28]M. Fink, "Time-reversal mirrors," J. Phys. D **26**, 1333 (1993).
[29]T. Ulrich, P. Johnson, and A. Sutin, "Imaging nonlinear scatterers applying the time reversal mirror," J. Acoust. Soc. Am. **119**, 1514–1518 (2006).
[30]P. Le Bas, K. Van Den Abeele, S. Dos Santos, T. Goursolle, and O. Bou Matar, "Experimental analysis for nonlinear time reversal imaging of damaged materials," Proc. of the ECNDT, Th. 4.6.3 (2006).
[31]A. Sutin, J. TenCate, and P. Johnson, "Single-channel time reversal in elastic solids," J. Acoust. Soc. Am. **116**, 2779–2784 (2004).
[32]S. Dos Santos and Z. Prevorovsky, "Imaging of human tooth using ultrasound based chirp-coded nonlinear time reversal acoustics," Ultrasonics **51**, 667–674 (2011).
[33]O. Matar, Y. Li, and K. Van Den Abeele, "On the use of a chaotic cavity transducer in nonlinear elastic imaging," Appl. Phys. Lett. **95**, 141913 (2009).
[34]K. Van den Abeele, P. Johnson, and A. Sutin, "Nonlinear elastic wave spectroscopy (NEWS) techniques to discern material damage. I. Nonlinear wave modulation spectroscopy (NWMS)," Res. Nondestruct. Eval. **12**, 17–30 (2000).
[35]L. Landau and E. Lifshitz, *Theory of Elasticity, Theoretical Physics*, 3rd ed. (Butterworth-Heinemann, Oxford, 1986), Vol. 7.
[36]J. B. Park and R. S. Lakes, *Biomaterials: An Introduction* (Springer, Berlin, 2007), Chap. 14.
[37]J.-G. Minonzio, J. Foiret, M. Talmant, and P. Laugier, "Impact of attenuation on guided mode wavenumber measurement in axial transmission on bone mimicking plates," J. Acoust. Soc. Am. **130**, 3574–3582 (2011).
[38]C. Leavens, R. Williams, F. S. Foster, P. N. Burns, and M. D. Sherar, "Golay pulse encoding for microbubble contrast imaging in ultrasound," UFFC IEEE **54**, 2082–2090 (2007).